Quasifree Proton-Proton and Proton-Deuteron Scattering on ^{3}He

D. R. Lehman*†

Center for Radiation Research, National Bureau of Standards, Washington, D. C. 20234
(Received 12 June 1972)

Quasifree proton scattering from ^{3}He is examined on the basis of available data. Cross sections are given in the pole-dominance approximation for either two protons or a proton and deuteron detected in coincidence. The cross sections are evaluated for a constant ^{3}He vertex and a separable-potential model of the ^{3}He vertex amplitude. Both two- and three-body breakup of ^{3}He are considered, with final-state rescattering included between the spectator nucleons in three-body breakup. It is shown that the asymptotic form of the coordinate-space ^{3}He wave function governs the shape of these low-momentum-transfer cross sections and that final-state rescattering between the spectator pair in ^{3}He$(p, 2p)pn$ mainly affects the magnitude of this cross section.

I. INTRODUCTION

The three-nucleon system has become important as a testing ground for phenomenological two-nucleon interactions and in extracting information about the structure of ^{3}He and ^{3}H.[1] Most investigations, both experimental and theoretical, deal with the three-nucleon system through its ground-state properties or through scattering processes which involve only three nucleons, e.g., n-d scattering or electron scattering from ^{3}He. In principle, it is possible to investigate the structure of ^{3}He and ^{3}H by bombarding them with strongly interacting particles, the simplest being protons (or neutrons). One objective in the initial stages of p-^{3}He scattering studies is to plan experiments whose interpretation does not require consideration of a four-body problem. This is achieved with coincidence experiments like ^{3}He$(p, 2p)$ and ^{3}He-(p, pd) under prescribed kinematic conditions.[2-4] The approach is to adjust the experimental parameters to correspond to quasifree scattering, i.e., low momentum transfer.

In this paper, we present a theoretical study of the recent ^{3}He$(p, 2p)$ and ^{3}He(p, pd) data.[2-4] Our objectives are twofold: (1) to determine what must be known about the ^{3}He wave function in order to interpret the data, and (2) to calculate the appropriate cross sections with wave functions derived from a separable-potential model of the two-nucleon interaction. We show that these experiments are mainly sensitive to the asymptotic form of the coordinate-space ^{3}He wave function and that final-state rescattering between the spectator pair in ^{3}He$(p, 2p)pn$ must be included to interpret the data.

The development begins in Sec. II with a brief justification of pole dominance and a derivation of the cross-section formulas. In Sec. III, the cross sections are computed assuming constant vertices and the relationship of this approximation to wave-function calculations is stressed. Sections IV and V contain, respectively, the separable-model calculations and the conclusions. An Appendix summarizes the kinematical considerations.

II. POLE DOMINANCE

The experiments under consideration differ in their incident proton energy, but are similar in that they all correspond to low momentum transfer, q. The incident proton energy determines the importance of initial-state, p-^{3}He rescattering corrections, which are greatest at low energies ($\lesssim 100$ MeV). The main effect of initial-state rescattering is to decrease the cross section without altering its shape.[3] Therefore, when this observation is combined with the low-momentum-transfer conditions, $q \lesssim 0.5$ fm^{-1}, a first attempt to understand the data can begin with the assumption that the amplitude is dominated by the pole diagram. A necessary, but not sufficient, condition for the applicability of the pole approximation is that $0 \leqslant q \lesssim K$, where $K^2/2\mu$ is the proton-deuteron binding in ^{3}He, with μ the p-d reduced mass.[5] For ^{3}He $\rightarrow p + d$, $K \approx 0.42$ fm^{-1}, and in the experiments, $q \lesssim K$, thus giving support to this approach. In this approximation, the derivations of the ^{3}He$(p, 2p)d$, ^{3}He$(p, 2p)pn$, and ^{3}He$(p, pd)p$ cross sections are similar, so we outline only the ^{3}He$(p, 2p)d$ case.

The ^{3}He$(p, 2p)d$ amplitude is calculated from the diagram in Fig. 1. The differential cross section averaged over initial spins and summed over final spins is

$$d\sigma = \frac{1}{V_{\text{rel.}}} \frac{1}{4} \sum_{i,f} |A_{fi}|^2 \delta^4(P_f - P_i) \frac{d^3q\, d^3k'_p\, d^3k''_p}{(2\pi)^5}, \quad (1)$$

where $V_{\text{rel.}}$ is the magnitude of the relative velocity of the incident proton and ^{3}He, $\frac{1}{4}$ comes from the spin averaging, the four-dimensional δ function requires over-all four-momentum conservation, and the meaning of the phase-space momentum variables is evident from Fig. 1. The amplitude A_{fi} in pole approximation is given by

$$A_{fi} = \sum_{\overline{m}_p} A^{3\text{He}}(\vec{q}; m_d \overline{m}_p, m) \frac{1}{(q^2/2M_p) - \epsilon - i\eta} A^{pp}(\vec{k}_p'' \vec{k}_p', \vec{q}\vec{k}_p; m_p'' m_p', \overline{m}_p m_p), \tag{2}$$

where $A^{3\text{He}}$ and A^{pp} are the ^{3}He $\rightarrow p + d$ and $p + p \rightarrow p + p$ vertex amplitudes, respectively. The m's represent the magnetic quantum numbers. A^{pp} is taken to be antisymmetric with respect to exchange of $(\vec{k}_p', m_p')$ and $(\vec{k}_p'', m_p'')$, thus assuring that the over-all amplitude is antisymmetric with respect to exchange of the two final-state protons. Conservation of energy at the ^{3}He vertex permits us to write the propagator as

$$\frac{q^2}{2M_p} - \epsilon \simeq \frac{3q^2}{4M_p} + B_2, \tag{3}$$

where B_2 is the p-d binding energy in ^{3}He($\hbar = c = 1$). We shall approximate the ^{3}He ground state by its dominant, spatially symmetric $^2S_{1/2}$ component. Thus, the ^{3}He $\rightarrow p + d$ vertex amplitude with its spin dependence displayed explicitly with a vector-coupling coefficient is

$$A^{3\text{He}}(\vec{q}; m_d \overline{m}_p, m) = A^{3\text{He}}(q)\langle 1 m_d \tfrac{1}{2} \overline{m}_p | \tfrac{1}{2} m \rangle \tag{4}$$

and $q = |\vec{q}|$. With Eq. (4), the spin sums can be done to get

$$\sum_{i,f} |A_{fi}|^2 = |A^{3\text{He}}(q)|^2 \frac{1}{[(3q^2/4M_p) + B_2]^2} \sum_{\substack{m_p \overline{m}_p \\ m_p' m_p''}} |A^{pp}(m_p'' m_p'; \overline{m}_p m_p)|^2. \tag{5}$$

When Eq. (5) is substituted into Eq. (1), the ^{3}He$(p, 2p)d$ cross section is

$$\frac{d\sigma}{d\Omega_p' d\Omega_p'' d\epsilon_p'} = \frac{|A^{3\text{He}}(q)|^2}{[(3q^2/4M_p) + B_2]^2} \frac{d\sigma(pp)}{d\tilde{\Omega}_p'} \times (\text{kinematic factor}) \tag{6}$$

and

$$\text{kinematic factor} = \frac{1}{(2\pi)^3} \frac{M_d k_p' k_p''^2 \overline{k}_p (\tilde{\epsilon}_p + \tilde{\epsilon}_p^q)^2}{M_p k_p \tilde{k}_p' \epsilon_p''} \left| \frac{k_p''}{\epsilon_p''} (\epsilon_d^q + \epsilon_p'') + \hat{k}_p'' \cdot (\vec{k}_p' - \vec{k}_p) \right|^{-1}. \tag{7}$$

The tilde, $\sim$, means in the p-p center-of-mass system and we have suppressed the q dependence of the p-p cross section. The kinematics, except for the exchanged proton, are treated relativistically. Thus, Eq. (6) is the general form of the ^{3}He$(p, 2p)d$ cross section in pole approximation.

The ^{3}He$(p, 2p)pn$ cross section is obtained from a diagram similar to the one in Fig. 1, except the spectator deuteron is replaced by a proton-neutron pair moving relative to each other with momentum $\vec{k}$. The phase-space volume in Eq. (1) has another factor, $d^3\kappa/(2\pi)^3$, and the ^{3}He vertex amplitude must be generalized to account for its dependence on $\vec{k}$ and the spin coupling, S, of the p-n pair. Equation (4) is replaced by

$$A_S^{3\text{He}}(\vec{q}, \vec{k}; m_{np} \overline{m}_p, m) = A_S^{3\text{He}}(\vec{q}, \vec{k})\langle S m_{np} \tfrac{1}{2} \overline{m}_p | \tfrac{1}{2} m \rangle \tag{8}$$

and the spin sums are done as before. The form of the cross section is

$$\frac{d\sigma(S)}{d\Omega_p' d\Omega_p'' d\epsilon_p'} = \frac{d\sigma(pp)}{d\tilde{\Omega}_p'} \frac{1}{(2\pi)^3} \int d^3\kappa \frac{|A_S^{3\text{He}}(\vec{q}, \vec{k})|^2}{[(3q^2/4M_p) + (\kappa^2/M_p) + B_3]^2} \times (\text{kinematic factor}), \tag{9}$$

where B_3 is the binding energy of ^{3}He. The kinematic factor has the same form as Eq. (7), but it now depends on κ and M_D is everywhere replaced by $M_p + M_n$. The range of the κ integration is determined from the kinematics and is discussed in the Appendix.

The remaining cross section, ^{3}He$(p, pd)p$, cannot be based on a single pole diagram if low-incident-proton energies ($\lesssim 50$ MeV) are to be considered. In addition to the usual diagram shown in Fig. 2, two other diagrams must be considered. The first comes from the antisymmetrization requirement for the two outgoing protons, which amounts to exchanging $-\vec{q}$ and $\vec{k}_p'$ in Fig. 2. The second arises from the neutron pickup process[6] shown in Fig. 3. These diagrams add coherently, and destroy the factorizability of the cross section in contrast to Eqs. (6) and (9). However, at high incident proton energies ($\gtrsim 100$ MeV) and low q, the contribution from the latter two processes should be negligible. The antisymmetrization diagram will

be suppressed due to the kinematic requirement of low q, while the neutron pickup diagram will be small due to the small $n + p \to d$ vertex amplitude at high energies, relative to the diagram in Fig. 2. Since we consider only the data at 587-MeV incident proton energy, the cross section is derived on the basis of Fig. 2.

The derivation of the $^3\mathrm{He}(p, pd)p$ cross section follows closely the $^3\mathrm{He}(p, 2p)d$ case. The notational changes in Eqs. (1) and (2) are obvious. The main difference in this derivation is the spin sums. They introduce a factor $\frac{2}{3}$, which combines with the $\frac{1}{4}$ in Eq. (1) to give $\frac{1}{6}$ – the necessary factor for the spin average in introducing the p-d cross section. The result is

$$\frac{d\sigma}{d\Omega_p' d\Omega_d' d\epsilon_p'} = \frac{|A^{3\mathrm{He}}(q)|^2}{[(3q^2/4M_p) + B_2]^2} \frac{d\sigma(pd)}{d\tilde{\Omega}_p'} \times (\text{kinematic factor}) \tag{10}$$

and

$$\text{kinematic factor} = \frac{1}{(2\pi)^3} \frac{M_p k_p' k_d'^2 \bar{k}_d (\bar{\epsilon}_p + \bar{\epsilon}_d)^2}{M_d k_p \bar{k}_d' \epsilon_d} \left| \frac{k_d'}{\epsilon_d'} (\epsilon_p^q + \epsilon_d') + \hat{k}_d' \cdot (\vec{k}_p' - \vec{k}_p) \right|^{-1}. \tag{11}$$

Equations (6), (9), and (10) are the basis of our discussions.

III. CONSTANT VERTICES

Thus far, two main approximations have been made in our discussion: (1) pole dominance; and (2) the $^3\mathrm{He}$ ground state is $^2S_{1/2}$. These assumptions led us to factorable forms of the coincidence cross sections. Our major concern in these expressions is the vertex amplitude, $A(q)$. The kinematic factors can be computed with the formulas given, but the p-p and p-d cross sections as expressed are not known, since they are "off-shell" cross sections, i.e., the exchanged particle is virtual. Since q is small ($q \lesssim 0.5$ fm^{-1}) in the experiments of interest, we introduce a third assumption: The exchanged particle is on shell. This corresponds to neglecting off-shell variations in the cross sections. We then substitute the on-shell p-p and p-d cross sections at the appropriate kinematical values. Usually, these cross sections are taken from experiment and thus introduce uncertainty into the computation

of the coincidence cross sections. This forms the framework within which $A(q)$ is studied.

We begin our investigation of $A(q)$ by assuming that it is independent of q. When $A(q)$ is taken to be a constant, the shape of the momentum distribution as a function of q obtained by dividing the coincidence cross section by the product of the kinematical factor and the p-p (p-d) cross section is determined by the propagator. This fact is a direct consequence of the pole-dominance approximation. We see in Figs. 4 and 5 (solid curves), that the shape of the momentum distributions is basically determined by the propagator for the $^3\mathrm{He}(p, 2p)d$ data at incident-proton energies of 35 and 155 MeV, respectively. At 155 MeV, we plot the coincidence cross section rather than the momentum distribution since the kinematic factor is a slowly varying function of q and the p-p cross section is taken to be a constant. The value of $|[(4M_p)/3]A^{3\mathrm{He}}|^2/(2\pi)^3$ used to set the normalization in each case is 3.5×10^{-2} fm^{-1} at 35 MeV and
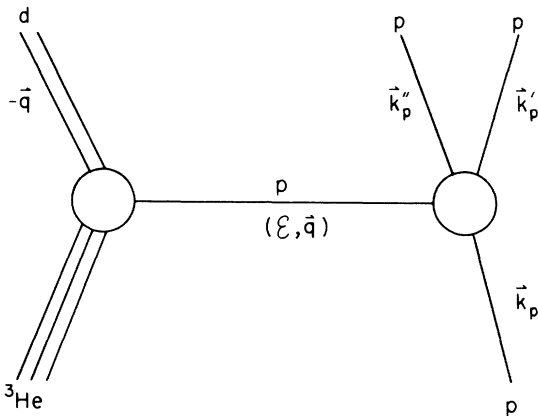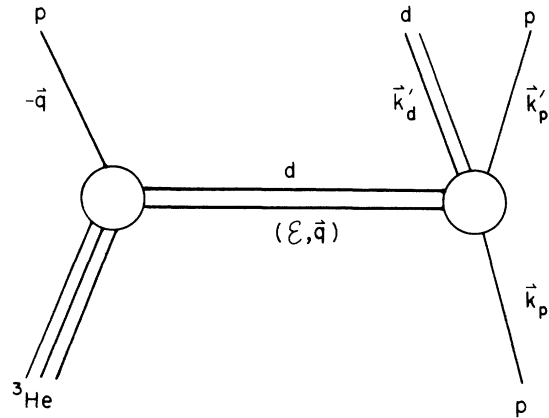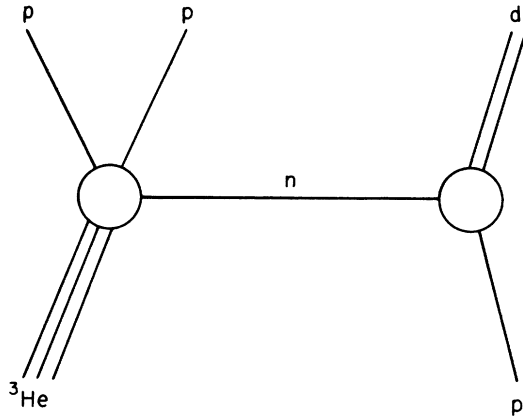

FIG. 1. $^3\mathrm{He}(p, 2p)d$ pole diagram.

FIG. 2. A $^3\mathrm{He}(p, pd)p$ pole diagram.

FIG. 3. Neutron-pickup diagram in ^{3}He$(p, pd)p$.

8.9×10^{-2} fm^{-1} for 155 MeV.[7] The difference in these values is a measure of the importance of initial-state rescattering (distortion) at the lower incident-proton energies.[8]

The vertex constant $|[(4M_p)/3]A^{3\text{He}}|^2/(2\pi)^3$ can also be extracted from the ^{3}He$(p, pd)p$ reaction. Data are available at both 35 and 587 MeV, but the 35-MeV data do not appear to be describable by the single diagram given in Fig. 2.[2] We mentioned above which additional diagrams most likely come into play, while Epstein et al.[6] have shown the significance of the neutron pickup diagram displayed in Fig. 3. Since the vertex constant has already been extracted from 35-MeV data, we consider only the 587-MeV data. Our curve in
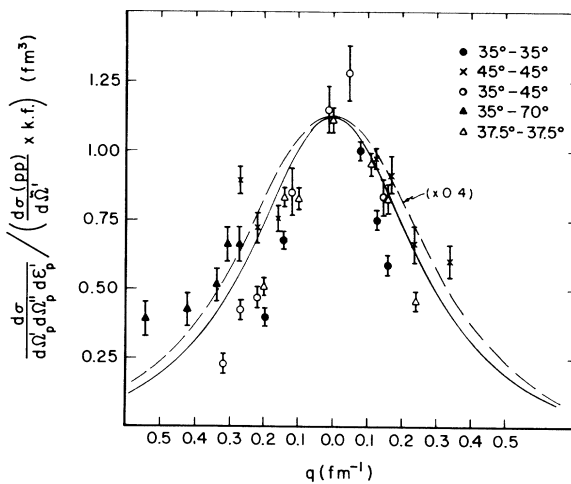

FIG. 5. ^{3}He$(p, 2p)d$ cross section at 155-MeV incident-proton energy. The solid curve is the constant-vertex result and the dashed curve is computed with the separable-potential model described in the text. The data are from Ref. 3.

Fig. 6 yields 7.1×10^{-2} fm^{-1} for the vertex constant.[9] This value is ~25% smaller than the value obtained at 155 MeV. We would have expected the 587-MeV result to be greater than that at 155 MeV, since initial-state rescattering should be negligible at 500–600-MeV incident energy. However, 25% is not a large difference and probably lies within present absolute experimental errors. Thus, with-

FIG. 4. ^{3}He$\rightarrow p + d$ momentum distribution at 35-MeV incident-proton energy. The solid curve is the constant-vertex result and the dashed curve is computed with the separable-potential model described in the text. The data are from Ref. 2.
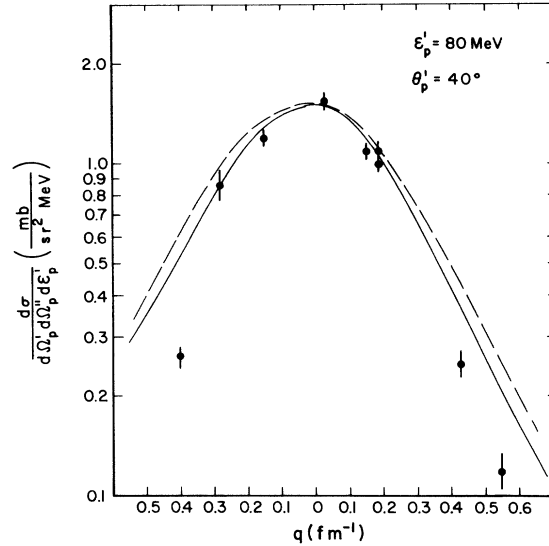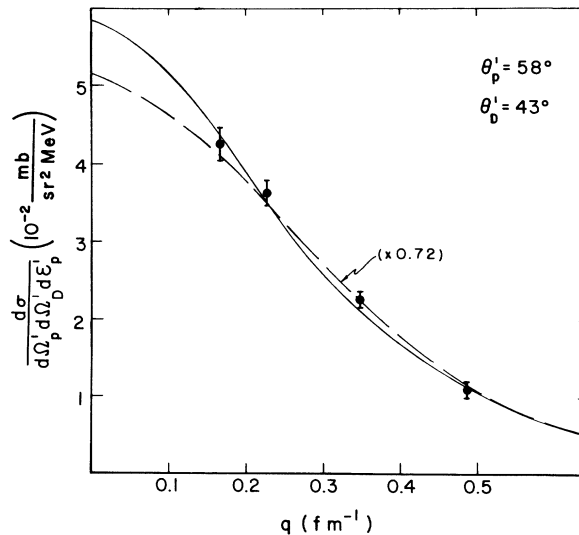

FIG. 6. ^{3}He$(p, pd)p$ cross section at 587-MeV incident-proton energy. The solid curve is the constant-vertex result and the dashed curve is computed with the separable-potential model described in the text. The data are from Ref. 4.

in these errors, the presently available data appear to be consistent.

We could go on and consider the ^{3}He$(p, 2p)pn$ reaction in the same way to extract the ^{3}He $\rightarrow p$ $+(pn)$ vertex constant, but our point about the shape is adequately served by the above discussion. The question which now arises concerns the meaning of this result with respect to wave-function calculations. First we establish how wave

functions come into play.

Wave-function calculations based on the Schrödinger equation are valid as long as the particles emerging from the ^{3}He vertex are nonrelativistic. The vertex amplitude, $A^{3\text{He}}(q)$, can then be computed if appropriate wave functions are available. As an example, consider the reaction ^{3}He$(p, 2p)d$. If particle 3 is taken to be the neutron, we can write the spatially symmetric $^2S_{1/2}$ ground state

of ^{3}He as

$$|^3\text{He}; \tfrac{1}{2}m\rangle = \psi_0(\overline{123})\chi_m^{[1/2]}(3, \hat{1}2), \tag{12}$$

where $\psi_0(\overline{123})$ is the spatial wave function symmetric under particle exchange and $\chi_m^{[1/2]}(3, \hat{1}2)$ is the total-spin-$\tfrac{1}{2}$ function antisymmetric under exchange of particles 1 and 2. The two-body p-d state in the ^{3}He vertex is

$$|p\text{D}; \vec{q}, m_d \overline{m}_p\rangle = \frac{1}{\sqrt{2}}\,\mathfrak{A}(\,g_{\vec{q}}(1, 23)\chi_{\overline{m}_p}^{[1/2]}(1)\chi_{m_d}^{[1]}(23))\,, \tag{13}$$

with $\mathfrak{A}$, the antisymmetrization operator for particles 1 and 2, and $g_{\vec{q}}(1, 23)$, the product of the deuteron wave function and a plane wave of momentum $\vec{q}$ for the proton-deuteron relative motion. The ^{3}He $\rightarrow p + d$ vertex amplitude is [See Eq. (4)]

$$A^{3\text{He}}(\vec{q}; m_d \overline{m}_p, m) = \langle\, pd; \vec{q}, m_d\,\overline{m}_p \,|\,V_{12}\,|^3\text{He}; \tfrac{1}{2}m\rangle \tag{14}$$

$$= -\left(\frac{3q^2}{4M_p} + B_2\right)\langle\, pd; \vec{q}, m_d\,\overline{m}_p \,|^3\text{He}; \tfrac{1}{2}m\rangle\,, \tag{15}$$

where V_{12} is the two-nucleon potential between particles 1 and 2. The Schrödinger equation was used in going from Eq. (14) to Eq. (15). When the spin sums are performed as before, the momentum distribution becomes

$$\frac{|A^{3\text{He}}(q)|^2}{[(3q^2/4M_p) + B_2]^2} = \frac{3}{2}\left|\int d^3r\, d^3\rho\, e^{-i\vec{q}\cdot\vec{\rho}}\varphi_B^*(r)\psi_0(\vec{r}, \vec{\rho})\right|^2 \tag{16}$$

or

$$= \frac{3}{2}(2\pi)^3\left|\int d^3k\,\varphi_B^*(k)\psi_0(\vec{k}, \vec{q})\right|^2. \tag{17}$$

$\varphi_B(r)$ is the coordinate-space, s-wave, deuteron wave function and its momentum space counterpart is $\varphi_B(k)$. The coordinates $\vec{r}$ and $\vec{\rho}$ are the standard Jacobi coordinates for three particles and all bound-state wave functions are normalized to unity. Thus the relationship of the vertex amplitude to wave functions is clear.

The answer to our question of wave-function interpretation can be established with Eq. (16). Since we are concerned with small values of q, the important contributions to the ρ integration come from ρ values $\gtrsim 2$ fm, thus emphasizing the asymptotic region of $\psi_0(\vec{r}, \vec{\rho})$ with respect to ρ. In this region, it is reasonable to take $\psi_0(\vec{r}, \vec{\rho})$ as the following factorizable form[10, 11]

$$\psi_0(\vec{r}, \vec{\rho})\xrightarrow[\rho \gtrsim 2\,\text{fm}]{} N\Phi(r)\frac{e^{-\beta\rho}}{\rho}\,. \tag{18}$$

It becomes clear immediately what the meaning of constant vertices is with respect to wave-function calculations, since the Fourier transform of $e^{-\beta\rho}/\rho$

is the propagator:

$$\int d^3\rho\, e^{-\vec{q}\cdot\vec{\rho}}\,\frac{e^{-\beta\rho}}{\rho} = \frac{4\pi}{\beta^2 + q^2}\,. \tag{19}$$

If $\beta^2 = 4M_p B_2/3$, we reproduce the constant-vertex result. The point is that the low-q experiments are mainly sensitive to the asymptotic region of the three-nucleon wave function; that region where one particle is relatively far removed from the remaining two. The major contribution to the amplitude comes from the external region in which there is only a weak nuclear interaction between the particles. This is the realm in which the pole approximation is valid.[12] Therefore, it is clear why the Irving-Gunn wave function, which behaves

asymptotically like Eq. (18), reproduces the shape of the data, but the Irving and Gaussian wave functions, which do not behave in this way, do not.[13] The exponential wave function behaves similarly to the Irving form, asymptotically.

We emphasize that the above discussion is predicated on two main conditions. Firstly, that the condition of pole dominance be satisfied: $q \lesssim \sqrt{2\mu B_2}$. Secondly, that the major effect of the initial-state rescattering corrections (distortion) is to reduce the magnitude of the cross section and not to alter its shape to any appreciable extent. There is sufficient evidence that this is the case.[3, 14, 15]

IV. SEPARABLE-POTENTIAL MODEL

In the previous section, we examined the general character of the low-momentum transfer ^{3}He$(p, 2p)$-d and ^{3}He$(p, pd)p$ data. We now consider the data with a model where the wave functions are derived from a parametrization of the two-nucleon interaction. This approach permits cross-section predictions to be made which are independent of other three-body data and the ^{3}He$(p, 2p)pn$ cross section to be computed in a consistent manner.

This model was used previously by the author for a study of quasielastic electron scattering from ^{3}He and ^{3}H.[16, 17] The two-nucleon interaction is represented by an s-wave, spin-dependent, separable potential of the Yamaguchi form.[18] The strength and range parameters are determined by fitting low to medium energy properties of the two-nucleon system.[19] The ground-state wave function of ^{3}He, which is taken to be the spatially symmetric $^2S_{1/2}$ component, is computed from an average of the singlet and triplet s-wave, two-nucleon interaction. This interaction gives 9.33 MeV for the three-nucleon binding energy. The corresponding wave function, when used to compute the charge radius, yields 1.75 fm for a proton charge radius of 0.80 fm. The charge-form-factor prediction agrees reasonably well with the data out to four-momentum transfer of ~4 fm^{-2}. Agreement is obtained with all the ^{3}He and ^{3}H quasi-elastic electrodisintegration data except the ^{3}He

coincidence data; this includes ^{3}He(e, e') and ^{3}H(e, e') at 248.8 and 398.4 MeV, and the tritium coincidence data, ^{3}H$(e, e'p)nn$. Further details and the values of the parameters used are given in Ref. 17.

Since a great deal of emphasis has been placed on the fact that the propagator essentially determines the shape of the coincidence data, we compare the separable-potential model ^{3}He$\to p + d$ momentum distribution with the constant vertex form and extract $|[(4M_p)/3]A^{3\text{He}}|^2/(2\pi)^3$. The two distributions are compared in Fig. 7 with the constant-vertex parameter determined to be 8.9×10^{-2} fm^{-1} from the separable-model distribution at $q = 0$. The curves have similar shapes and in the region of maximum difference, ~0.2 to ~0.5 fm^{-1}, differ by 15–20%. If the separable-model value of B_2, 7.10 MeV, is used in the propagator of the constant-vertex calculation, the shape of the resulting momentum distribution is indistinguishable from that of the separable-model distribution. Therefore, a ^{3}He wave function with a binding energy closer to the experimental value would be expected to give a higher value at $q = 0$ and a shape essentially the same as the propagator form calculated with the experimental binding energy.

Comparison of the separable-model to the constant-vertex case indicates what to expect when comparing the separable model to the ^{3}He$(p, 2p)d$ and ^{3}He$(p, pd)p$ results. At 35 MeV, we predict the ^{3}He$(p, 2p)d$ momentum distribution to have roughly the shape of the data, but it is a factor 2.5 too high. The 155-MeV prediction has its maximum at the same value as the data, but does not reproduce the shape of the data as q increases beyond 0.2 fm^{-1}. For ^{3}He$(p, pd)p$ at 587 MeV, the separable model is ~40% too high. These results are shown as the dashed curves in Figs. 4–6.

The only ^{3}He$(p, 2p)pn$ data published to date are at 155 MeV.[3] We compute the cross section on the basis of Eq. (9), with the ^{3}He$\to p + (pn)^S$ vertex determined by the separable-model wave functions. The cross section comes from the incoherent sum of two amplitudes: one where the spectator pair is coupled to singlet spin and the other, triplet spin. The momentum distribution is

$$\frac{\sum\limits_{S=0}^{1}|A_S^{3\text{He}}(\vec{q}, \vec{k})|^2}{[(3q^2/4M_p)+(\kappa^2/M_p)+B_3]^2} = (2\pi)^3 \left\{ \frac{1}{2} \left| \int d^3k \, \varphi_{\vec{\kappa},0}^{(-)*}(\vec{k})\psi_0(\vec{k}, \vec{q}) \right|^2 + \frac{3}{2} \left| \int d^3k \, \varphi_{\vec{\kappa},1}^{(-)*}(\vec{k})\psi_0(\vec{k}, \vec{q}) \right|^2 \right\}, \quad (20)$$

where $\varphi_{\vec{\kappa},s}^{(-)}(\vec{k})$ is the spin-s, incoming wave, two-nucleon scattering wave function in momentum space. When only the plane-wave part of $\varphi_{\vec{\kappa},s}^{(-)}(\vec{k})$ is used in Eq. (20), this means the final-state rescattering between the spectator particles is neglected. To demonstrate the importance of the rescattering, we compute both cases. The results[7] are shown in Fig. 8. The cross-hatched region around $q = 0$ is kinematically inaccessible (see Appendix). The plane-wave calculation yields a cross section more than a factor of two higher than the calculation which includes the rescattering.[20] Also, the shape of the plane-wave curve

is different than the rescattering curve. Atten-
tion should be given to the small contribution of
the triplet rescattering by comparing the full re-
scattering curve (singlet plus triplet) with the
singlet rescattering curve (triplet contribution
set equal to zero). Moreover, the factor of four
difference between the ^{3}He(p, $2p$)d and ^{3}He(p, $2p$)-
pn cross sections is roughly reproduced. These
two results combined reflect the relative impor-
tance of the p-d, p-$(pn)^{S=0}$, and p-$(pn)^{S=1}$ wave
function overlaps with the ^{3}He ground state. The
p-d overlap is the most important, while the
p-$(pn)^{S=1}$ overlap is of least importance. This
result is compatible with the fact that the d and
$(pn)^{S=1}$ wave functions are orthogonal. The factor
of 4 difference between the ^{3}He(p, $2p$)d and ^{3}He-
(p, $2p$)pn cross sections can thus be attributed
mainly to the d being more like the (pn) pairing
in ^{3}He than the $(pn)^{S=0}$ is. It should also be men-
tioned that though a large portion of the p-$(pn)^{S=0}$
overlap comes from the region of low relative (pn)
momentum, it is not concentrated at zero relative
(pn) momentum. The maximum relative energy of
the spectator (pn) pair ranges from ~5 MeV at
$q = 0.1$ fm^{-1} to ~30 MeV at $q = 0.5$ fm^{-1}.

V. CONCLUSIONS AND DISCUSSION

The survey of the available p-^{3}He coincidence
data presented above draws us to three conclu-
sions: (1) The shape of the coincidence cross sec-
tions is predominantly describable by the pole
mechanism with a constant ^{3}He vertex. In a non-
relativistic Schrödinger-equation description of
the ^{3}He vertex, this means only the large-distance

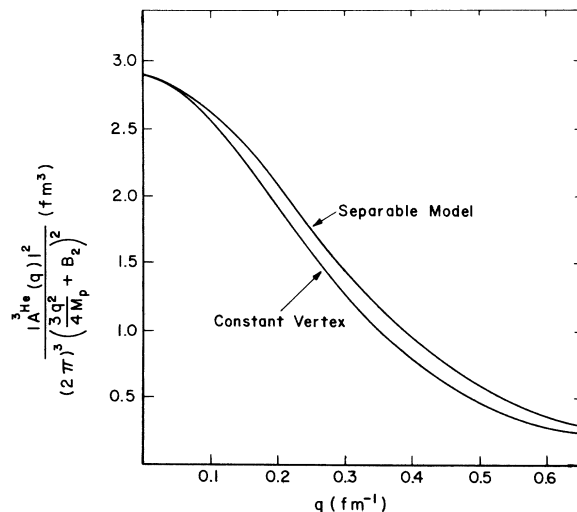behavior of the ^{3}He wave function is being tested
in low-momentum transfer experiments. (2) Final-
state rescattering between the spectator pair in
the ^{3}He(p, $2p$)pn reaction is very important. In-
clusion of the rescattering reduces the calculated
cross section more than a factor of two compared
to letting the spectator particles move freely rela-
tive to one another. This is an indication of the
relative importance of the various wave function
overlaps with the ^{3}He ground state. For example,
the p-d overlap with ^{3}He is large compared with
the p-$(np)^{S=1}$ overlap. (3) Initial-state rescatter-
ing (distortion) is important, especially at the
lower energies. This is seen by comparing the
constant-vertex values of the 35- and 155-MeV
data, and the result from Ref. 3 that the effect
reduces the cross section by 25–30% at 155 MeV.

As more experimental data of this type become
available, the consistency of the data at different
energies can be checked by extracting the ^{3}He
vertex constants in the approximation of a constant
^{3}He vertex. If the initial-state rescattering cor-
rections are included, the extracted vertex con-
stants should all be the same. Thus, the problem
of including the initial-state rescattering corre-
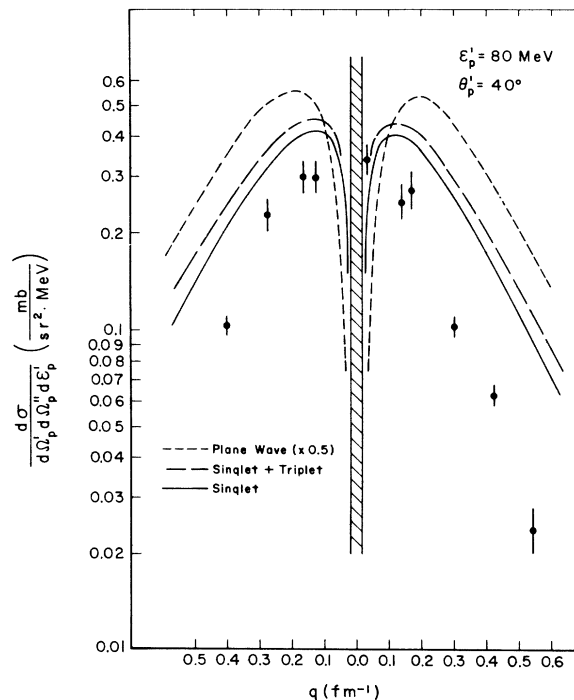sponding to diagrams like those in Fig. 9 will

FIG. 7. Comparison of constant-vertex and separable-
model momentum distributions at low-momentum transfer.

FIG. 8. ^{3}He(p, $2p$)pn cross section at 155-MeV incident-
proton energy. The curves are computed with the separ-
able-potential model described in the text. The data are
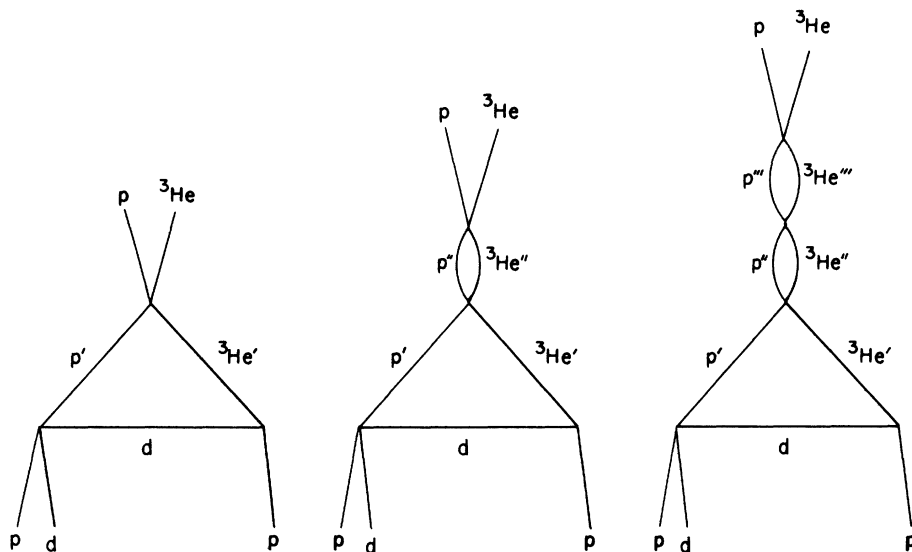from Ref. 3.

FIG. 9. Initial-state rescattering diagrams.

become more important. One way of including this effect is through the conditions of unitarity and dispersion relations.[21] This leads to an equation of the Omnes-Muskhelishvilli type. Either from elastic p-^{3}He data or an appropriate model, the necessary amplitudes (phase shifts) can be inserted and the initial-state rescattering effects computed.

It is desirable to begin obtaining data for a larger range of q. At the same time, however, it is very important to determine when the pole-dominance approximation is no longer valid. That is, by means of the Treiman-Yang test when it is applicable,[22, 23] determine at what q this breakdown occurs. This is crucial to determining what must be understood as more sensitivity to the ^{3}He wave function is gained. Of course as q becomes larger, off-shell effects in the p-p and p-d vertices become more important. However, the question remains whether these experiments are really sensitive to these effects and whether off-shell effects can be studied in this way.

Finally, there is always the question of Coulomb effects which manifest themselves in numerous ways; ^{3}He replaced by ^{3}H or (p, pn) instead of ($p, 2p$). Nevertheless, progress in these investigations depends on what complications arise and how they can be handled to maximize the extraction of information about ^{3}He and the two-nucleon interaction. One must not lose sight of the fact that this work is on the edge of the four-body problem.

ACKNOWLEDGMENTS

The author's interest in this subject developed

through correspondence with Dr. J. C. Alder and later, with Dr. C. F. Perdrisat, and he is grateful to both. He would also like to thank Dr. M. Danos, Dr. A. Ghovanlou, Dr. J. S. O'Connell, and Dr. F. Prats for beneficial discussions.

APPENDIX: KINEMATICS

As an example of the kinematical relations involved, we consider the ^{3}He($p, 2p$)d and ^{3}He($p, 2p$)-np reactions at 155 MeV. Conservation of four-momentum yields three kinematical equations:

$$\epsilon_p + \epsilon_{^3\text{He}} = \epsilon_q^d + \epsilon_p' + \epsilon_p'' + \left(\frac{\kappa^2}{M_p}\right), \qquad (A1)$$

$$k_p = q\cos\theta_q + k_p'\cos\theta_p' + k_p''\cos\theta_p'', \qquad (A2)$$

$$0 = q\sin\theta_q + k_p'\sin\theta_p' - k_p''\sin\theta_p''. \qquad (A3)$$

The notation is defined in Fig. 1 and Sec. II, and the angles are referred to the incident-proton direction in the laboratory. The parenthetical term arises only when the deuteron is disintegrated. In that case, ϵ_q^d is replaced by ϵ_q^{np}.

The fixed quantities in the experiment are $k_p(\epsilon_p)$, $k_p'(\epsilon_p')$, and θ_p', while θ_p'' is varied. This leaves three unknowns, $q(\epsilon_q^d)$, θ_q, and $k_p''(\epsilon_p'')$, with three equations to determine them. As θ_p'' varies from 28 to 72°, q decreases from 0.528 fm^{-1} to zero and then increases again to 0.855 fm^{-1}.

The case where the deuteron is disintegrated introduces another unknown into the kinematics – the relative momentum of the spectator pair, κ. To compute the cross section, an integral over the appropriate range of κ must be performed. The maximum value, κ_{max}, is determined by the fact that for fixed q, κ increases at the expense of

$k_p''(\epsilon_p'')$ [see Eq. (A1)]. Therefore, the minimum value of k_p'' allowed by Eqs. (A2) and (A3) is determined, and then κ_{max} from Eq. (A1).

It is straightforward to show that, for the conditions of the Orsay experiment, q has a minimum value, $q_{min} \neq 0$, in the ^{3}He$(p, 2p)pn$ case. An important observation is that as $q \rightarrow q_{min}$, $\kappa_{max} \rightarrow 0$. Thus, the range of κ integration becomes smaller and smaller, until finally, q_{min} is reached. Then

the cross section is zero. This is the explanation of the sharp drop in the calculated ^{3}He$(p, 2p)pn$ cross section as q_{min} is approached. (q_{min} was computed to be ~0.018 fm^{-1} for the Orsay experiment.)

All transformations from laboratory to center-of-mass quantities and for computing appropriate energies at the p-p and p-d vertices were done using relativistically invariant expressions.

*National Academy of Science—National Research Council postdoctoral research associate.

†Present address: Department of Physics, The George Washington University, Washington, D. C. 20006.

[1]R. D. Amado, Ann. Rev. Nucl. Sci. 19, 61 (1969); L. M. Delves and A. C. Phillips, Rev. Mod. Phys. 41, 497 (1969); A. N. Mitra, in *Advances in Nuclear Physics*, edited by M. Baranger and E. Vogt (Plenum, New York, 1969), Vol. III, p. 1; A. G. Sitenko and V. F. Kharchenko, Usp. Fiz. Nauk 103, 469 (1971) [transl.: Soviet Phys.-Usp. 14, 125 (1971)].

[2]I. Šlaus, M. B. Epstein, G. Paić, J. R. Richardson, D. L. Shannon, J. W. Verba, H. H. Forster, C. C. Kim, D. Y. Park, and L. C. Welch, Phys. Rev. Letters 27, 751 (1971).

[3]R. Frascaria, V. Comparat, N. Marty, M. Morlet, A. Willis, and N. Willis, Nucl. Phys. A178, 307 (1971).

[4]P. Kitching, G. A. Moss, W. C. Olsen, W. J. Roberts, J. C. Alder, W. Dollhopf, W. J. Kossler, C. F. Perdrisat, D. R. Lehman, and J. R. Priest, Phys. Rev. C 6, 769 (1972).

[5]I. S. Shapiro, Usp. Fiz. Nauk 92, 549 (1967) [transl.: Soviet Phys.-Usp. 10, 515 (1968)].

[6]M. B. Epstein, I. Šlaus, D. Shannon, J. R. Richardson, J. W. Verba, H. H. Forster, C. Kim, and D. Y. Park, Phys. Letters 36B, 305 (1971).

[7]For the p-p cross section in the 155-MeV case, we use 3.64 mb/sr. The p-p cross section is essentially constant at this value for laboratory energies between 170 and 430 MeV, and center-of-mass scattering from 20 to 90°. W. N. Hess, Rev. Mod. Phys. 30, 368 (1958). In the 35-MeV case, Ref. 2, the p-p cross section and kinematic factor have already been divided out.

[8]The vertex constant computed here is related to the reduced vertex part. I. S. Shapiro, Nucl. Phys. 28, 244 (1961).

[9]The p-d cross section for 587-MeV incident protons, scattered at 90° in the center of mass, is based on the data of J. S. Vincent, W. K. Roberts, E. T. Boschitz, L. S. Kisslinger, K. Gotow, P. C. Gugelot, C. F. Perdrisat, L. W. Swenson, and J. R. Priest, Phys. Rev. Letters 24, 236 (1970). The value is 0.050±0.002 mb/sr.

[10]E. L. Slaggie and E. H. Wichmann, J. Math. Phys. 3, 946 (1962).

[11]J. M. Knight, J. S. O'Connell, and F. Prats, Phys. Rev. 164, 1354 (1967).

[12]Similar points were made in Appendix C of Ref. 17.

[13]The forms of these wave functions are given in Ref. 3.

[14]M. Morlet, R. Frascaria, B. Geoffrion, N. Marty, B. Tatischeff, and A. Willis, Nucl. Phys. A129, 177 (1969).

[15]D. F. Jackson and B. K. Jain, Phys. Letters 27B, 147 (1968).

[16]D. R. Lehman, Phys. Rev. Letters 23, 1339 (1969).

[17]D. R. Lehman, Phys. Rev. C 3, 1827 (1971); ibid C 4, 1010(E) (1971).

[18]Y. Yamaguchi, Phys. Rev. 95, 1628 (1954).

[19]F. Tabakin, Phys. Rev. 137, B75 (1965).

[20]This was the case in our ^{3}He(e,e') and ^{3}H(e,e') work also. However, it was not made clear in Ref. 17 that curves (B) in Figs. 10 and 11 included only the contribution from the plane waves with singlet spin. The triplet-spin plane-wave part must be included as well.

[21]I. S. Shapiro, in *Selected Topics in Nuclear Theory*, edited by F. Janouch (International Atomic Energy Agency, Vienna, 1963), p. 85.

[22]S. B. Treiman and C. N. Yang, Phys. Rev. Letters 8, 140 (1962).

[23]I. S. Shapiro and V. M. Kolybasov, Nucl. Phys. 61, 353 (1965).